buildings

MDPI

Article

Production of Glass Foam in a Microwave Oven Using Agro-Industrial Waste as Raw Material

Fernando Antonio da Silva Fernandes [1,2,*], Thamara Fernanda da Silva Fernandes [3] and João Adriano Rossignolo [2]

[1] Department of Engineering (FAE), Federal University of Pará, Campus Salinópolis, Rua Raimundo Santana Cruz, S/N, Bairro São Tomé, Salinópolis 68721-000, PA, Brazil
[2] Department of Biosystems Engineering, University of São Paulo, USP, Av. Duque de Caxias Norte, 225, Pirassununga 13635-900, SP, Brazil; rossignolo@usp.br
[3] Faculty of Medicine, Federal University of Pará, Rua Augusto Correa, 01—Guamá, Belém 66075-110, PA, Brazil; thamara.fernandes@ics.ufpa.br
* Correspondence: fernandofernandes@ufpa.br

Abstract: Climate change is characterized by shifts in temperature and climate patterns. Constructing new high-rise environments using materials that incorporate agro-industrial waste can help mitigate this impact without compromising technological properties. This study produced vitreous foams intended to replace natural aggregates in lightweight concrete partially. These foams were sintered in a microwave oven at temperatures of 750 °C, 800 °C, and 850 °C, utilizing glass powder and sugarcane bagasse ash as raw materials. The homogenization and preparation of these materials were conducted through a mechanical pelletization process, employing a constant rotation engine at approximately 40 rpm. The efficacy of microwave sintering was assessed by comparing the outcomes with those from sintering in a conventional electric muffle furnace under identical conditions. The results indicated that the microwave-sintered vitreous foams exhibited the following values for apparent density ($\leq$0.30 g/cm^3), porosity (86% to 94%), and compressive strength (0.48 MPa to 0.58 MPa), which align with the global standards for commercial vitreous foams. The microwave sintering route proved to be economically feasible by reducing sintering time and, consequently, energy costs, without sacrificing technological properties. The materials produced in this study offer a promising solution to minimize the environmental impact associated with constructing new buildings, particularly tall structures. Additionally, they support the circular economy by converting waste into valuable by-products.

Keywords: circular economy; sustainability; lightweight concrete; lightweight aggregate; density; ash; glass

Citation: Fernandes, F.A.d.S.; Fernandes, T.F.d.S.; Rossignolo, J.A. Production of Glass Foam in a Microwave Oven Using Agro-Industrial Waste as Raw Material. *Buildings* **2024**, *14*, 1643. https://doi.org/10.3390/buildings14061643

Academic Editors: Antonio Caggiano and Shahid Azam

Received: 12 April 2024
Revised: 30 April 2024
Accepted: 22 May 2024
Published: 3 June 2024

1. Introduction

Climate change, a key driver behind the shifts in temperature and weather patterns globally, significantly impacts human health and quality of life [1–3]. Numerous studies have explored strategies to mitigate or eliminate environmental damage. However, everyone must recognize the impossibility of meeting present needs at the expense of future generations.

Burning plant waste such as sugarcane bagasse releases carbon dioxide (CO_2), a major greenhouse gas, into the atmosphere, contributing to global warming. This process also emits particulate matter and pollutants like carbon monoxide, nitrogen oxides, and volatile organic compounds, which can deteriorate air quality and human health. Additionally, these emissions can indirectly influence climate change by affecting cloud formation and the absorption of solar radiation.

A potential solution lies in developing the Blue Economy, which encourages a capitalist society to enhance sustainability across all facets, particularly through the promotion of

cleaner energy sources [4]. In this scenario, the Circular Economy emerges as a viable model. It emphasizes the recovery and utilization of food waste [5], promotes the use of renewable resources, and supports the recycling of waste into new materials, thereby keeping them in the economic loop far longer than traditionally expected [6–8]. This approach not only extends the life cycle of materials but also significantly reduces pollution from production processes and improper disposal, effectively decoupling economic growth from environmental degradation [6].

The construction sector significantly contributes to the development of the global economy but also imposes a substantial environmental burden. This burden primarily arises from its high energy consumption, significant emissions that contribute to the greenhouse effect, and the generation of vast amounts of solid waste [9,10]. The global trend towards building taller structures has escalated concrete production, making it the most utilized material worldwide [11–14], with annual production nearing 10 billion cubic meters [15]. Research has indicated that construction processes can integrate various waste materials into concrete, such as vitreous foams [7,8], bamboo fibers [16], PET bottles [17], and glass bottles [18], to mitigate environmental impacts.

Vitreous foams, in particular, have gained attention in the construction industry for their desirable attributes, such as lightweight, rigidity, and high compressive strength [19–22], alongside being effective thermal insulators [23]. These foams are fabricated using a base of recycled glass powder [24], with soda-lime glass—a type constituting 90% of global glass production—being a primary material [15,25]. This glass category is chemically stable and softens at approximately 800 °C [26].

Agricultural by-products, such as sugarcane bagasse ash (SCBA) from the cogeneration of energy in sugar and alcohol-producing plants, provide a sustainable silica source for glass powder without compromising its properties [27,28]. With Brazil, India, and China leading in sugarcane production, a significant portion of the crop residue ends up as ash. Despite its high silica content, which is advantageous for vitreous foam production, this ash is underutilized and often disposed of in landfills [28–33].

In the manufacture of vitreous foams, calcium carbonate ($CaCO_3$) is an effective and economical foaming agent [33]. It decomposes at temperatures between 650 °C and 1000 °C [7,34], producing CaO and CO_2, with the latter playing a crucial role in pore formation, as it is trapped within the glass matrix during the molten phase [15,35]. CaO aids in lowering the viscosity of the melt, and during the casting phase, it reduces the resistance to pore growth, allowing for volumetric expansion. This reduced viscosity enhances oxygen transfer, which facilitates the oxidation of carbon within the cellular structure, thereby increasing the gas content [36]. The sintering process significantly affects the technological properties of vitreous foams [34,37,38].

New sintering techniques could make the production of vitreous foams for industrial use more economically viable. An innovative approach is sintering using a microwave oven, which has shown greater energy efficiency due to the shorter processing times at high temperatures compared to traditional sintering methods [39–41]. Microwave sintering emerges as a compelling alternative to conventional high-temperature treatment techniques [39,41]. The process conducted in the microwave oven enhances volumetric expansion and mechanical properties while reducing the apparent density—a crucial characteristic of commercial glass foams [15,24,40–43].

This study focused on producing vitreous foams sintered in a microwave oven to partially substitute natural aggregate in concrete [7,8,15]. Compared to conventional sintering methods, this new sintering route is more efficient as it reduces sintering time and, consequently, energy costs, offering economic advantages in the production of the vitreous foams under investigation. Raw materials such as soda-lime glass powder, SCBA, and calcium carbonate were selected to further decrease production expenses. Vitreous foams boast technological properties such as compressive resistance, low density, and minimal water absorption. Notably, this material does not require mixing with water, thereby avoiding competition with concrete hydration.

The glass foams produced in this study can serve as a lightweight aggregate to partly replace conventional aggregate. Manufacturing this novel product through a cost-effective process helps minimize waste disposal associated with this research, converting it into valuable co-products. Moreover, this approach aligns with the principles of the circular economy and promotes revenue generation through the sale of waste.

2. Materials and Methods

The methodology of the manuscript is presented in the subsequent sections. The steps, procedures, and techniques used in the research are described in detail, ensuring transparency and reproducibility of the results obtained. The experimental flow of this investigation is illustrated in Figure 1.

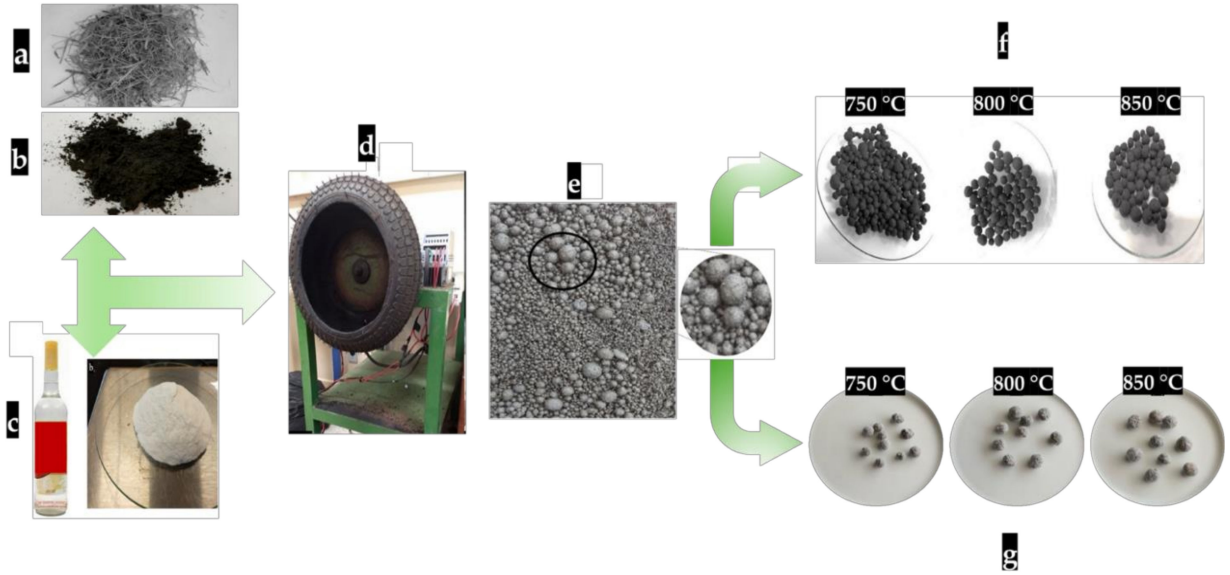

Figure 1. (**a**) Sugarcane bagasse, (**b**) SCBA, (**c**) glass powder, (**d**) pelletizing machine, (**e**) pellets in green state, (**f**) vitreous foam sintered in a conventional electric muffle furnace, and (**g**) vitreous foam sintered in a microwave oven.

2.1. SCBA

The SCBA used in this study was obtained from the sugarcane grinding process for ethanol production and energy generation at Usina Bunge, located in Pedro Afonso, TO, Brazil (8°58′4″ S; 48°10′30″ W), as depicted in Figure 1b. The sugarcane bagasse (Figure 1a) underwent washing, cleaning of residual impurities, and drying at room temperature, followed by oven drying at 100 °C for 48 h. The bagasse was then manually cut into approximately 5 mm sizes. Subsequently, it was incinerated in an electric muffle furnace at a temperature of 900 °C, at a heating rate of 100 °C/min [7,8,44] (Figure 1b).

Sintering in the laboratory was conducted to achieve the same temperature that produced the SCBA used in this study. The SCBA was sieved using a 150 mesh ABNT sieve (106 μm), and the material that passed through underwent particle size distribution analysis using a laser particle size analyzer (CILAS 1180). A sample sintered at each temperature was selected, pulverized, and analyzed by X-ray diffraction (XRD) (Shimadzu, Tokyo, Japan).

2.2. Glass POWDER

The glass used in this study was obtained from transparent bottles typically utilized as beverage containers (Figure 1c). The bottles were washed and oven-dried before being manually crushed to yield particles <10 mm. These particles were further processed in a ball mill [11] (TS RUBENS, São Paulo, Brazil) at a speed of 100 rpm with steel grinding bodies (36.5; 30.2; 25.4; 19.1; 15.9 mm) until they were fine enough to pass through a

150 ABNT standard mesh sieve (106 µm). The milling time was not regulated. Following the methodology described in [7], the material that passed through the sieve was then analyzed for particle size distribution using a laser particle size analyzer (CILAS 1180).

2.3. $CaCO_3$

Industrial-grade calcium carbonate ($CaCO_3$) manufactured by Dinâmica (São Paulo, SP, Brazil) (23°33′1″ S; 46°38′2″ W) was utilized as a foaming agent because of its proven efficiency [7,8,15,45,46] and economic viability [26]. The material underwent particle size distribution analysis using a laser particle size analyzer (CILAS 1180).

2.4. Production of Vitreous Foams

The technological properties of the samples sintered at 750 °C, 800 °C, and 850 °C in both a conventional electric muffle furnace and a microwave oven were examined. A mass formulation consisting of 78% glass powder, 16% SCBA, and 6% $CaCO_3$ was used for the analysis. This formulation was proved successful in a previous study conducted by the first author [15]. The specific formulation is detailed in Table 1.

Table 1. Formulation investigated.

Sample	Material (%)		
	Glass powder	SCBA	$CaCO_3$
	78	16	6

2.5. Pre-Test

Before sintering (Figure 1e), the samples underwent preliminary testing to determine the ideal binder for producing the vitreous foams. Four binders were evaluated: starch (Maizena®), a polyfunctional water-reducing plasticizing additive (MIRA® SET) according to the (ABNT: NBR 11768/201), PVA, and clay (provided by Cerâmica Reunidas, Cristalândia, TO, Brazil) (10°36′14.7″ S; 49°11′56.0″ W). Three samples from each formulation were tested to assess their behavior at various sintering temperatures in a conventional electric muffle furnace (750 °C, 800 °C, and 850 °C).

2.6. Pelletizing

The formulated samples (referenced in Table 1) underwent a granulation process employing the mechanical pelletization method (illustrated in Figure 1d) for approximately 5 min, with the motor rotating at about 40 rpm. Throughout the pelletizing process, water (5%) was manually sprayed, accompanied by the addition of 5% PVA (Polyvinyl Alcohol P.S, Dinâmica, São Paulo, Brazil) [47], resulting in the production of pellets ready for sintering [18,47].

2.7. Sintering of Samples

The samples underwent the sintering process identically in both a conventional electric muffle furnace and a microwave oven, following the temperature ranges explored in this study and previous research [7,39]. The authors of these works produced vitreous foams by sintering in both a microwave oven and a conventional electric muffle furnace at temperatures ranging from 700 °C to 1000 °C. For conventional sintering, an electric muffle furnace (EDG 1800, Rio de Janeiro, Brazil) was used, following a sintering cycle of 100 °C/h and a 30 min sintering time [8,34]. Microwave sintering was performed in a 1000 W oven (SHARP R-8720, Chicago, MA, USA), using a hybrid approach. A silicon carbide susceptor was placed inside the chamber to achieve a heating rate of 50 °C/min [39].

2.8. Characterization of Vitreous Foams

Volumetric Expansion

The volumetric expansion of the samples sintered in both an electric muffle furnace and a microwave oven was measured through Equation (1). This involved calculating the mass of the sample before sintering, following pelletization and drying (in ambient conditions), to determine its initial volume (V*i*). The post-sintering volume (V*f*) was ascertained by immersing the sample in a beaker filled with pentane petals (>180 µm) to a pre-measured volume [15]. To ensure accuracy, this process was repeated three times. The increase in the height of the pentane indicated a volume change, from which the volumetric expansion of the vitreous post-sintering foam was calculated through Equation (2).

$$\mathrm{V}i = \pi.r^2.h, \tag{1}$$

where V*i* = initial volume, *r* = base radius, and *h* = height.

$$Expansion = \left(\frac{vf - vi}{vi}\right) \times 100 \tag{2}$$

where V*i* represents the volume of the sample after forming and drying, measured in grams per cubic centimeter (g/cm^3), and V*f* denotes the volume after sintering, also in g/cm^3.

The volume determined through the displacement method within the beaker, combined with the mass obtained from weighing the vitreous foam post-sintering, enabled the calculation of density through Equation (3).

$$\rho = \frac{m}{v} \tag{3}$$

where m is the mass (g) and v is the volume (cm^3) of the vitreous foam.

2.9. Porosity

The total porosity (ϵ%) of the foams, whether sintered in a conventional electric muffle furnace or a microwave oven, was calculated through Equation (4). This calculation is based on the comparison between the apparent density (ρa) of the sintered foam and the theoretical density (ρt) of the initial powders.

$$\varepsilon(\%) = \left[1 - \frac{\rho_a}{\rho_t}\right] \tag{4}$$

The apparent density of the samples was calculated based on their mass and geometric dimensions.

The internal architecture and formation of pores were visualized by examining cross-sectional images captured by an optical microscope (Olympus, 3Z61, Taiyuan, China).

2.10. Water Absorption

The water absorption of the vitreous foam samples, whether sintered in a conventional electric muffle furnace or a microwave oven, was measured following the procedures outlined in the technical (ABNT-NBR NM 53:2009)—Coarse aggregate—Determination of specific mass, apparent specific mass, and water absorption, as specified by Equation (5).

$$A = \frac{ms - m}{m} \times 100 \tag{5}$$

where A represents the water absorption percentage, m_s is the mass of the sample in air when in a saturated surface-dry condition (g), and m is the mass of the dry sample in air (g).

2.11. Compressive Strength

The uniaxial compressive strength of the vitreous foam, sintered in both a conventional electric muffle furnace and a microwave oven, was determined for samples with a particle size retained on a 12.5 mm sieve (ABNT-NBR NM-ISO 3310-1:1997). Compression tests were conducted using a universal testing machine (EMIC, model DL-2000), at a crosshead speed of 10 mm/min, adhering to the (ASTM C133–97R15, 2015 standard). Five samples from each sintered vitreous foam formulation were assessed for compressive strength, ensuring compliance with the granulometric specification of 12.5 mm, as required by this standard. Given the samples' non-standard geometric shapes and their interface with the loading cell, 2 mm thick EVA (ethylene-vinyl acetate) plates were utilized to achieve homogeneous load transfer and compensate for any surface irregularities [15,48].

2.12. Granulometry

The granulometric analysis of the vitreous foams produced in this study was conducted using a sieve set, adhering to the specifications outlined in the (ABNT-NBR 7211:2009), specifically employing a 12.5 mm mesh for retaining the material [7,15].

3. Results and Discussion

3.1. Granulometry

The results concerning the grain size of the raw materials (Table 2) indicate that the grain size favored the production of vitreous foams in this investigation, regardless of the sintering temperature or method. This effect may have been enhanced by the pelletizing process of the raw materials before sintering, where smaller grains occupy the empty spaces between larger grains, filling potential voids that might arise. The average size of the SCBA grains (102.77 µm) likely makes a significant contribution, as the glass powder must incorporate the SCBA during its liquid phase to form the cellular structure of the foam during sintering [15].

Table 2. Granulometry: SCBA—Glass powder—$CaCO_3$.

Material	D_{10}	D_{50}	D_{90}	$D_{average}$
			(µm)	
SCBA	26.20	100.28	175.64	102.77
Glass powder	7.21	44.12	94.00	48.33
$CaCO_3$	1.15	2.39	4.86	2.74

3.2. Chemical Composition

Table 3 presents the results of the chemical composition of the raw materials investigated, where SCBA predominantly contains SiO_2 (55.52%) [39], and the glass powder consists of soda-lime glass [38]. The chemical composition of $CaCO_3$ predominantly features CaO (97.77%), which is typical for industrialized $CaCO_3$ [7,8,45].

Table 3. Chemical composition: SCBA, glass powder, and $CaCO_3$.

Material	Composition *						
	SiO_2	CaO	Na_2O	AI_2O_3	K_2O	Fe_2O_3	P_2O_5
SCBA	55.52	8.99	4.78	2.67	5.67	-	0.99
Glass powder	72.26	12.01	12.61	1.48	0.87	0.77	0.36
$CaCO_3$	0.40	97.77	-	0.06	-	0.14	1.09

* Expressed in oxides. MnO, MgO, SrO, and SO_3 were found in smaller proportions.

3.3. Binding Agent

The results of the preliminary test to determine the binding material are illustrated in Figure 2. The binding materials investigated were starch (Maizena®), a polyfunctional

water-reducing plasticizer additive (MIRA® SET), PVA, and clay. The results show the values of volumetric expansion of the vitreous foams relative to the sintering temperature in a conventional electric muffle furnace and the type of binder used. PVA demonstrated the highest efficiency at all temperatures tested, with volumetric expansion ranging from 160% to 320%, followed by starch (45–170%), the superplasticizer (45–145%), and clay (35–125%). The effectiveness of PVA as a binder was anticipated, as this material has been previously utilized in several other studies [7,8,15,39,43,49].

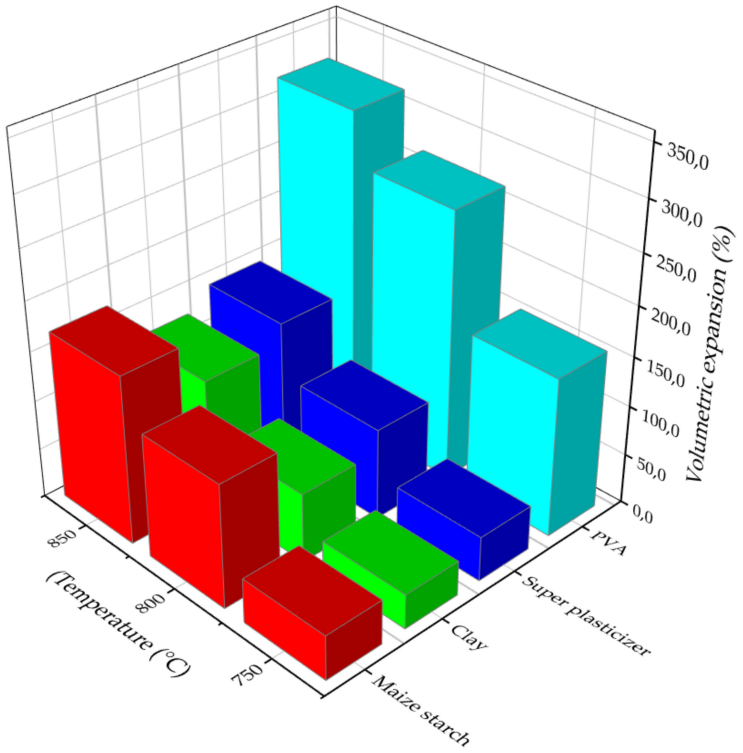

Figure 2. Volumetric expansion of the vitreous foam concerning the type of binder by sintering temperature in a conventional electric muffle furnace.

3.4. Sintering

The sintering of the vitreous foams produced in this study in both a conventional electric muffle furnace and a microwave oven favored volumetric expansion, regardless of the method used. This condition was supported by the formulation (Table 1), and the result was expected, as this formulation has been previously tested. The external geometric shapes of the samples sintered in a conventional electric muffle furnace and a microwave oven are illustrated in Figures 3 and 4, respectively.

Figure 3. Geometric shape of vitreous foams sintered in an electric muffle furnace: (**a**) 750 °C, (**b**) 800 °C, and (**c**) 850 °C.

Figure 4. Geometric shape of vitreous foams sintered in a microwave oven: (**a**) 750 °C, (**b**) 800 °C, and (**c**) 850 °C.

Visual assessment (within the field of view) of the external geometric shape (pellets) of the vitreous foams, as shown in Figures 3 and 4, after sintering in a conventional electric muffle furnace and a microwave oven, respectively, reveals that their geometries are similar regardless of the sintering method. There is no significant variation in the apparent density values, which is a crucial characteristic. This similarity can be attributed to the formulation, the pelletizing process, and the grain size of the raw materials, which were consistent across samples. The predominance of SiO_2 (55.52%) in the SCBA may have played a role in the formation of the cellular structure during the liquid phase of the glass powder. The formation of the internal architecture of the pores in the foams sintered in a conventional electric muffle furnace and a microwave oven is illustrated in Figures 5 and 6, respectively.

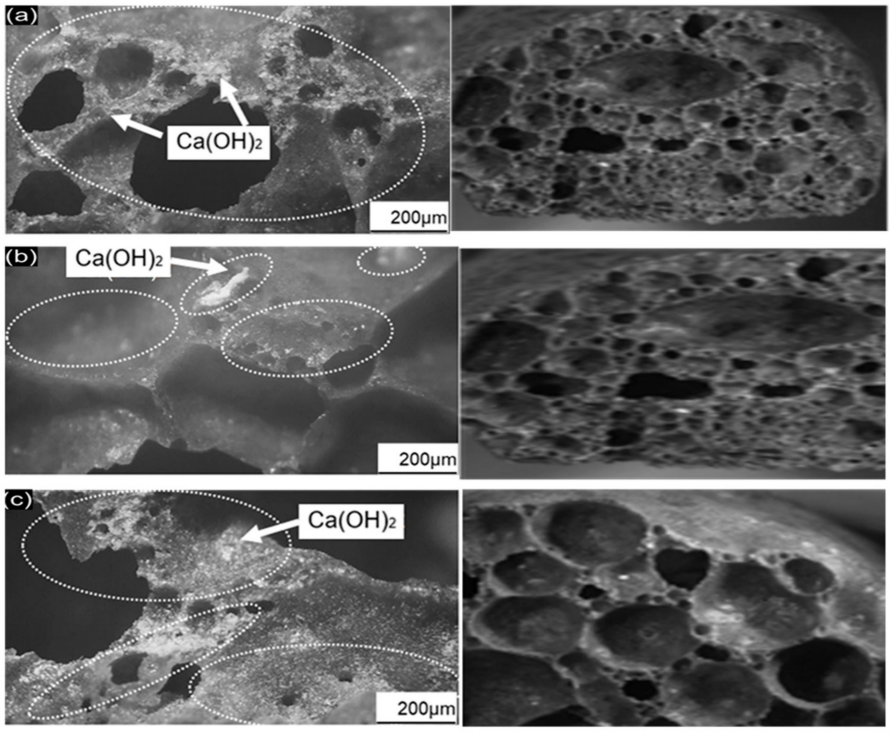

Figure 5. Formation of the architecture and geometric shape of the pores of vitreous foams sintered in a conventional electric muffle furnace: (**a**) 750 °C, (**b**) 800 °C, and (**c**) 850 °C.

From visual inspection (Figures 5 and 6), it is evident that the vitreous foams sintered in both a conventional electric muffle furnace and a microwave oven exhibit no cracks on their internal walls. Instead, they feature uniformly distributed pores with closed porosity and very similar morphology. The porosity of the samples, ranging from 85% to 91%, was likely enhanced by the decomposition of $CaCO_3$ into CaO, which acted as a modifier for

the silicate networks. This process reduced the viscosity of the molten silicate material by breaking SiO_2 tetrahedra [22], leading to the formation of larger pores or those connected with microspores [36,50]. The similarity in pore architecture could also be linked to the effectiveness of the binding material, the pelletization process, and the influence of $CaCO_3$. According to the results, $CaCO_3$ contributed to increased porosity due to its decomposition at high temperatures [22,51].

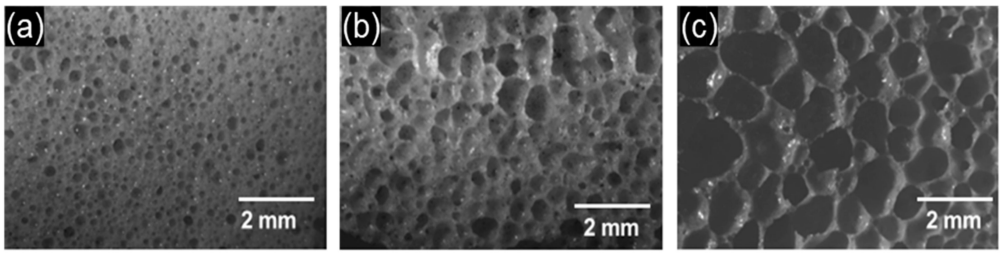

Figure 6. Formation of the architecture and geometric shape of the pores of vitreous foams sintered in a microwave oven: (**a**) 750 °C, (**b**) 800 °C, and (**c**) 850 °C.

Visually, within the observation area, a difference in pore size is notable. This non-uniform pore structure is attributed to the temperature of foam formation during the molten liquid phase [22,51,52]—a result of the gradual temperature increase which significantly affects the size and formation of pores [15,53]. As temperature rises, $CaCO_3$ decomposes more, generating new gases, primarily CO. These gases, initially trapped within the pores, begin to escape as the temperature continues to rise and pressure inside the pore increases. This process allows the gases to break through the internal walls, interconnecting the pores and forming the internal architecture of the vitreous foam [15,54]. Observing Figure 6, the formation of calcium hydroxide ($Ca(OH)_2$) can be seen, likely resulting from prolonged sintering in a conventional electric muffle furnace.

When sintering in a microwave oven, the absence of $Ca(OH)_2$ is notable, attributed to the unique energy transfer process during microwave sintering. This process involves the conversion of energy from electromagnetic fields into molecular kinetic energy, which is then transformed into heat [55]. This method differs fundamentally from sintering in a conventional electric muffle furnace because of the nature of heat transfer [42]. Microwave energy—as electromagnetic energy operating at frequencies ranging from 0.3 to 300 GHz—enables a distinctive heating mechanism. As microwaves penetrate and move through dielectric materials, they interact with molecular dipoles. This interaction creates an electric field that reorients these dipoles to align with the fluctuating electromagnetic field. Despite the continuous change in the electromagnetic field, leading to a phase difference between the field and the dipoles, the dipoles undergo random collisions. These collisions result in energy loss, which is subsequently converted into thermal energy.

The optical microscopy results depicted in Figure 7 confirm the observed resemblance between Figures 5 and 6, illustrating the needle-shaped crystals. Furthermore, Figures 7 and 8 reveal areas that appear relatively flat, with minor fractures at different elevations. These plane fractures bear resemblance to the cleavage fractures often observed in many ceramics [56]. Microwave sintering, as depicted in Figure 6, results in isolated pores, which contribute to a decrease in water absorption [39,42]. This characteristic of vitreous foams sintered in a microwave oven is crucial for their application as lightweight aggregate materials in construction, particularly beneficial in high-rise buildings [7]. Additionally, a homogeneous distribution of pores, observed in the same figure, could enhance compression resistance.

The specific geometric shape of the vitreous foams (pellets) produced in this study, characterized by closed pores, is advantageous for incorporating into lightweight concrete. This is because the cement paste cannot infiltrate the foam's pores, thereby preventing paste loss and reducing the need for additional cement to achieve proper adhesion [15]. Moreover, this geometric shape assists in occupying the voids between natural aggregates, thus improving the compressive strength of lightweight concrete by filling these

gaps with vitreous foams, which contributes to concrete strength as it leaves fewer voids subject to stress.

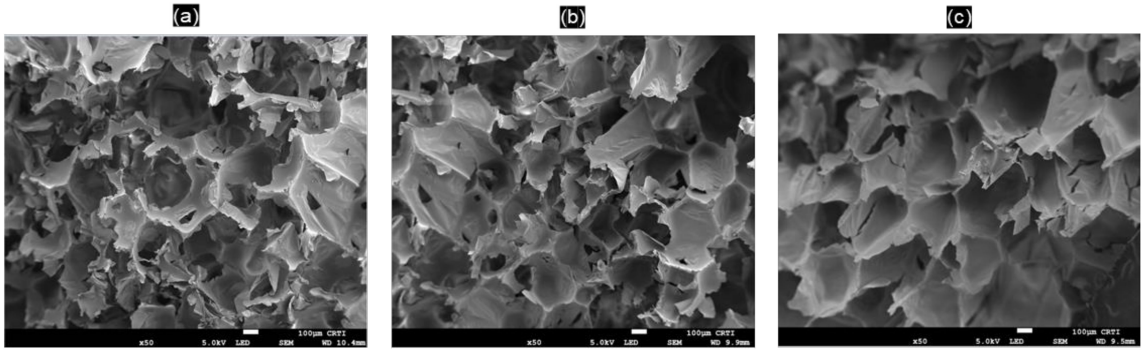

Figure 7. Optical microscopy images of the vitreous foams sintered in an electric muffle furnace: (**a**) 750 °C, (**b**) 800 °C, and (**c**) 850 °C.

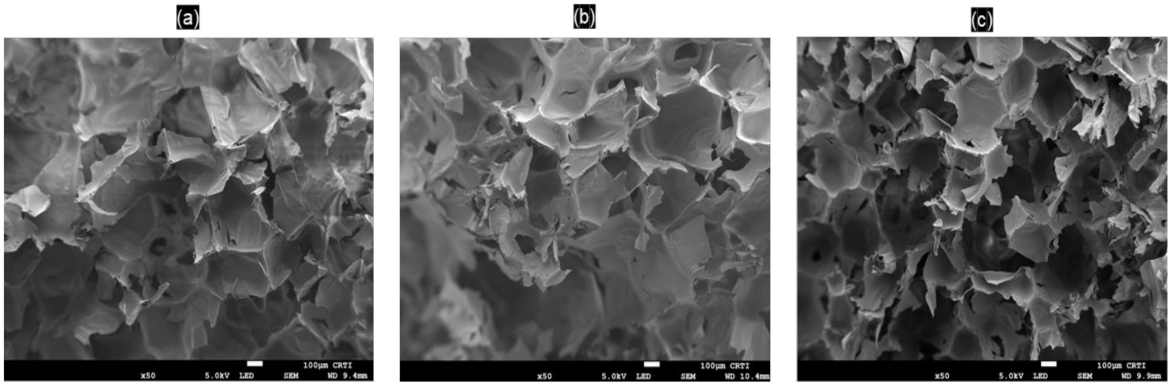

Figure 8. Optical microscopy images of the vitreous foams sintered in a microwave oven: (**a**) 750 °C, (**b**) 800 °C, and (**c**) 850 °C.

The formation of these structures was also significantly influenced by the average particle size of the raw materials (Table 2). The average grain size of $CaCO_3$ (2.74 µm) played a vital role in the stability and formation of the internal cellular structure, as $CaCO_3$ acts as a flux, ensuring a structure dominated by closed pores. This results in low or negligible permeability, which competes with the cement's hydration reactions for the mixing water [15,57,58].

Sintering vitreous foams at temperatures between 750 °C and 850 °C in a microwave oven also helps lower the production costs of this material, facilitating its manufacturing and wider adoption in the construction sector through innovative production techniques [15,26,59]. The vitreous foams developed in this study are tailored to meet the specific requirements of lightweight concrete [7,35,60]. Their porosity, pore size, and compressive strength values are detailed in Table 4.

The vitreous foams sintered in both a conventional electric muffle furnace and a microwave oven were sorted using an sieve (12.5 mm), with the observed porosity ranging from 86% to 94%. This range indicates a relative similarity, likely facilitated by consistent sintering temperatures and formulations across different sintering methods. Despite variations in the sintering temperatures, the values were closely aligned, underscoring the effectiveness of the chosen temperatures for processing the vitreous foams produced in this study [15,24,34,49]. A slight increase in porosity was noted (as shown in Figures 6c and 7c) at a temperature of 850 °C, which likely contributed to the formation of larger pores due to the gas release from $CaCO_3$ sintering at this temperature.

Table 4. Porosity, pore size, and compressive strength of vitreous foams.

	Description	Temperature (°C)		
		750	800	850
Conventional electric muffle furnace	Porosity (%)	85 ± 2	87 ± 2	91 ± 2
	Pore size (mm)	1.2 ± 1	1.6 ± 1	2.1 ± 1
	Compressive strength	0.58 ± 0.02	0.55 ± 0.02	0.51 ± 0.02
	Description	**Temperature (°C)**		
		750	**800**	**850**
Microwave oven	Porosity (%)	86 ± 2	86 ± 2	94 ± 2
	Pore size (mm)	1.32 ± 1	1.69 ± 1	2.28 ± 1
	Compressive strength	0.62 ± 0.02	0.61 ± 0.02	0.59 ± 0.02

Pore sizes were measured between 1.32 mm and 2.28 mm, with no significant differences observed across samples sintered at varying temperatures. The presence of larger pores is attributed to the porosity resulting from the decomposition of $CaCO_3$ at temperatures conducive to glass expansion. Conversely, smaller pores are thought to arise from newly nucleated pores by CO_2 that did not expand significantly.

The mechanical compressive strength of the vitreous foams was found to be between 0.48 and 0.58 MPa. Given their relatively uniform porosity and pore size, the vitreous foams sintered at from 750 °C to 800 °C are expected to exhibit similar mechanical resistance to compression. It is noteworthy that commercial vitreous foams generally present compressive strength ranging from 0.4 to 6 MPa for porosity levels >70% (Scheffler, 2005). Hence, the vitreous foam spheres produced in this study satisfy the fundamental requirements for commercial vitreous foams.

3.5. Density—Water Absorption

The results for the apparent density and water absorption of vitreous foams sintered in both a conventional electric muffle furnace and a microwave oven are depicted in Figure 9a,b. All values for density and water absorption met the expected criteria. The density values (≤0.30 g/cm^3) align perfectly with those of commercial vitreous foams produced globally [18,35,57,60]. These findings underscore the potential impact of the vitreous foams developed in this study on the construction industry, particularly concerning the 'wet' of lightweight concrete. The wet refers to the mass per unit volume of fresh concrete, which is primarily influenced by the type and quantity of materials used in the concrete mix [61].

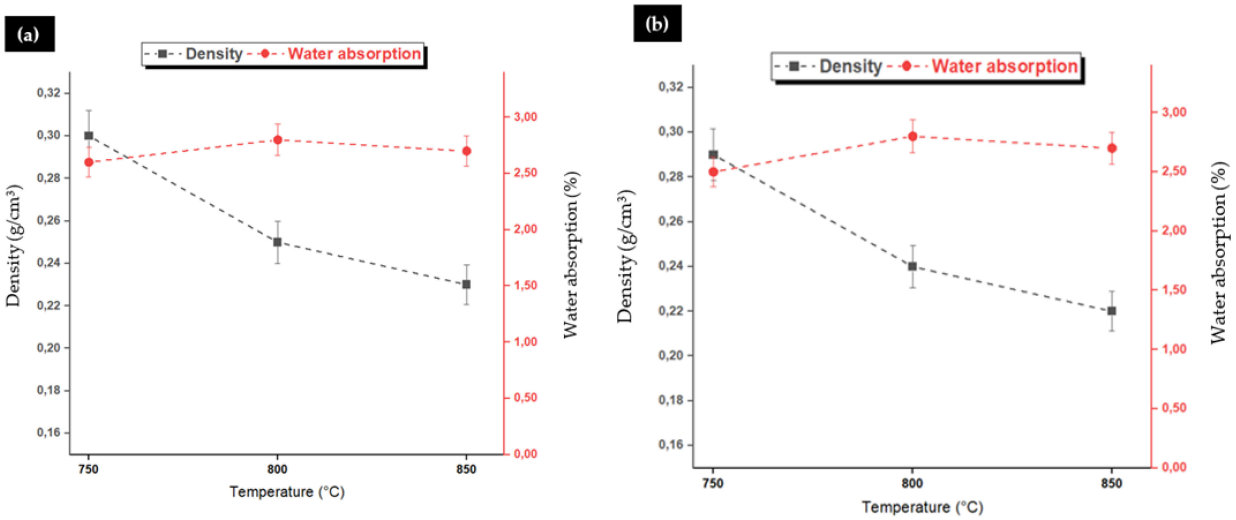

Figure 9. (**a**). Density and water absorption values of vitreous foams sintered in a conventional electric muffle furnace. (**b**). Density and water absorption of vitreous foams sintered in a microwave oven.

3.6. X-ray Diffraction (XRD)

The results depicted in Figure 10, related to the XRD analysis, clearly indicate the amorphous nature of the samples. This suggests a significant influence from the high concentration of the vitreous phase when sintered at 750 °C, 800 °C, and 850 °C. Crystalline phases, identified by the presence of cristobalite (SiO_2) and wollastonite ($CaSiO_3$), are clearly visible because of the excessive presence of silica in SCBA (55.52%) and glass powder (72.26%). Additionally, the $CaCO_3$ shows a high content of CaO (97.77%).

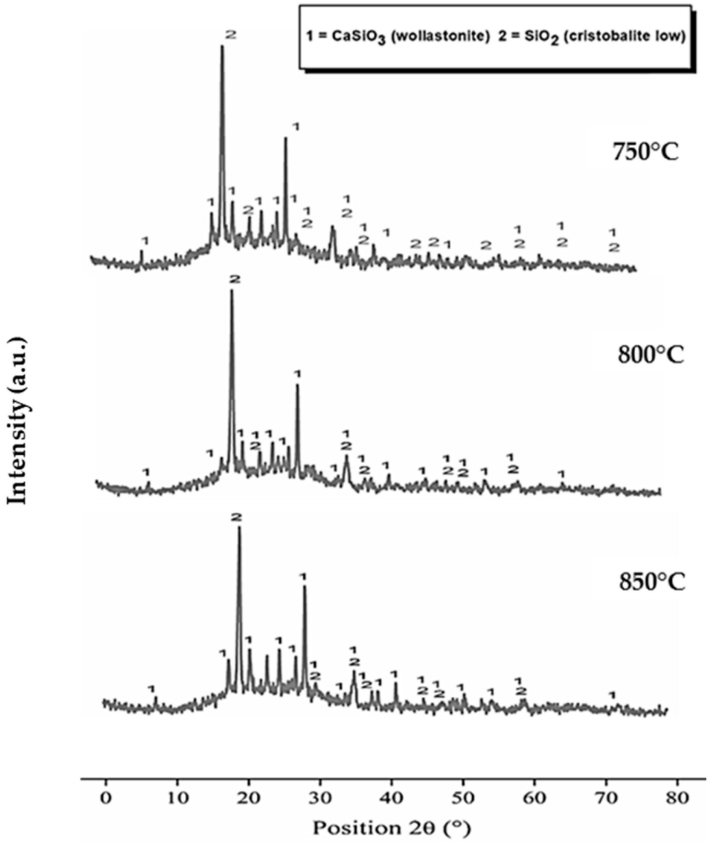

Figure 10. XRD patterns of samples sintered at 750 °C, 800 °C, and 850 °C in a microwave oven.

Some silicas were not incorporated into the cellular structure of the foams during their formation in the vitreous phase, resulting in calcium hydroxide ($Ca(OH)_2$), which only appeared in samples sintered in a conventional electric muffle furnace [62,63]. This confirms the strong influence of temperature on the formation of the cellular structure of this material.

The presence of the crystalline phase raises concerns about the potential for devitrification of the foams during their manufacturing process, as devitrification can negatively influence the crystallization process during the formation of the cellular structure, affecting the properties and formation of the vitreous foam [62].

These findings highlight the reactive nature of SCBA within the structure of soda-lime glass and suggest that residual carbon was sintered, promoting the crystallization of amorphous silica ash into cristobalite. This transformation was anticipated, as the sintering temperatures used are conducive to the formation of this specific silica phase, although the peak intensities indicate a system that retains significant amorphism.

3.7. Sintering Time

In this study, it was found that the microwave oven demonstrated the highest energy efficiency for sintering, reaching temperatures of 750 °C in 4 min, 800 °C in 6 min, and 850 °C in 8 min. In contrast, the conventional electric muffle furnace required an average of

12 h to achieve the same temperature levels (750 °C, 800 °C, and 850 °C). This significant reduction in processing time results in substantial energy savings. These findings align with those of previous studies that have confirmed the technical and economic feasibility of using microwave ovens for industrial-scale, high-temperature processes [39,40]. The reduced sintering time not only optimizes the manufacturing process of glass foams but also enhances the sintering quality and the overall technological characteristics of the product [64].

4. Conclusions

The results of this study confirm that using waste materials—specifically glass powder, sugarcane bagasse ash, and calcium carbonate as a foaming agent—to produce glass foams is both technologically and economically viable when sintered in a microwave oven at temperatures of 750 °C, 800 °C, and 850 °C. The properties achieved, such as apparent density ($\leq$0.30 g/cm^3), porosity (86–94%), and compressive strength (0.59–0.62 MPa), align well with the standards of commercial foams produced globally. Microwave oven sintering proves highly efficient, processing materials from the inside out in significantly less time than conventional electric muffle furnaces.

Sugarcane bagasse ash is effectively integrated into the cellular structure of the glass powder during its liquid phase, enhancing the formation of closed pores. Calcium carbonate also demonstrates high efficacy as both a pore-forming agent and a fluxing material.

Moreover, the utilization of agro-industrial waste—78% glass powder and 16% sugarcane bagasse ash—not only adds value but also transforms the waste into a by-product, promoting the principles of the circular economy within small communities.

Author Contributions: F.A.d.S.F., T.F.d.S.F. and J.A.R.; formal analysis, F.A.d.S.F. and J.A.R.; investigation, F.A.d.S.F. and J.A.R.; methodology, F.A.d.S.F., T.F.d.S.F. and J.A.R.; resources, F.A.d.S.F. and J.A.R.; writing—original draft preparation, F.A.d.S.F., T.F.d.S.F. and J.A.R.; writing—review and editing, F.A.d.S.F. and J.A.R.; visualization, F.A.d.S.F., T.F.d.S.F. and J.A.R. All authors have read and agreed to the published version of the manuscript.

Funding: This research received no external funding.

Data Availability Statement: The data presented in this study are available on request from the corresponding author.

Acknowledgments: This study was supported for publication by PROPESP/UFPA (PAPQ).

Conflicts of Interest: The authors declare no conflicts of interest.

References

1. Pope, C.A., III. Lung Cancer, Cardiopulmonary Mortality, and Long-Term Exposure to Fine Particulate Air Pollution. *JAMA* **2002**, *287*, 1132–1141. [CrossRef] [PubMed]
2. Pandolfi, P.; Notardonato, I.; Passarella, S.; Sammartino, M.P.; Visco, G.; Ceci, P.; De Giorgi, L.; Stillittano, V.; Monci, D.; Avino, P. Characteristics of Commercial and Raw Pellets Available on the Italian Market: Study of Organic and Inorganic Fraction and Related Chemometric Approach. *Int. J. Environ. Res. Public Health* **2023**, *20*, 6559. [CrossRef] [PubMed]
3. Wang, X.; Lv, G.; Zhang, Y.; Yu, Y.; Wang, X.; Peixoto, L.; Qian, C.; Pang, H. Annual Burying of Straw after Pelletizing: A Novel and Feasible Way to Improve Soil Fertility and Productivity in Northeast China. *Soil Tillage Res.* **2023**, *230*, 105699. [CrossRef]
4. Vassallo, L.; Appolloni, A.; Fantauzzi, C.; Frondizi, R. Reducing Plastic Pollution by Recovery and Recycling: Evidence from a "Blue Economy" Project Impacting Policy-Making in Italy. *Int. J. Environ. Res. Public Health* **2023**, *20*, 5604. [CrossRef]
5. Cárdenas, J.; Orjuela, A.; Sánchez, D.L.; Narváez, P.C.; Katryniok, B.; Clark, J. Pre-Treatment of Used Cooking Oils for the Production of Green Chemicals: A Review. *J. Clean. Prod.* **2021**, *289*, 125129. [CrossRef]
6. Apostu, S.A.; Gigauri, I.; Panait, M.; Martín-Cervantes, P.A. Is Europe on the Way to Sustainable Development? Compatibility of Green Environment, Economic Growth, and Circular Economy Issues. *Int. J. Environ. Res. Public Health* **2023**, *20*, 1078. [CrossRef]
7. Fernandes, F.A.d.S.; Costa, D.d.S.d.O.; Martin, C.A.G.; Rossignolo, J.A. Vitreous Foam with Thermal Insulating Property Produced with the Addition of Waste Glass Powder and Rice Husk Ash. *Sustainability* **2023**, *15*, 796. [CrossRef]
8. da Silva Fernandes, F.A.; de Oliveira Costa, D.d.S.; Rossignolo, J.A. Influence of Sintering on Thermal, Mechanical and Technological Properties of Glass Foams Produced from Agro-Industrial Residues. *Materials* **2022**, *15*, 6669. [CrossRef]
9. Barros, A.; Barreira, E.; Maia, L.; Lopes, M.L. Incorporation of Waste in Thermal Mortars—A Literature Review. *Buildings* **2024**, *14*, 830. [CrossRef]

10. Liu, B.; Gao, Q.; Liang, L.; Sun, J.; Liu, C.; Xu, Y. Ecological Relationships of Global Construction Industries in Sustainable Economic and Energy Development. *Energy* **2021**, *234*, 121249. [CrossRef]
11. Liu, X.; Jiang, T.; Li, C.; Wan, M.; Xuan, W.; Wang, X. Effect of Precursor Blending Ratio and Rotation Speed of Mechanically Activated Fly Ash on Properties of Geopolymer Foam Concrete. *Buildings* **2024**, *14*, 841. [CrossRef]
12. Fernandes, F.A.d.S.; Barbar, J.S.; Costa, D.d.S.d.O.; Rossignolo, J.A. Experimental Investigation on Interfacial Defect Detection for SCCS with Different Contact NDT Technical. *Buildings* **2023**, *13*, 2549. [CrossRef]
13. Getachew, E.M.; Yifru, B.W.; Taffese, W.Z.; Yehualaw, M.D. Enhancing Mortar Properties through Thermoactivated Recycled Concrete Cement. *Buildings* **2023**, *13*, 2209. [CrossRef]
14. Hosseinnezhad, H.; Sürmelioğlu, S.; Çakır, Ö.A.; Ramyar, K. A Novel Method for Characterization of Recycled Concrete Aggregates: Computerized Microtomography. *J. Build. Eng.* **2023**, *76*, 107321. [CrossRef]
15. da Silva Fernandes, F.A.; Arcaro, S.; Tochtrop Junior, E.F.; Valdés Serra, J.C.; Bergmann, C.P. Glass Foams Produced from Soda-Lime Glass Waste and Rice Husk Ash Applied as Partial Substitutes for Concrete Aggregates. *Process Saf. Environ. Prot.* **2019**, *128*, 77–84. [CrossRef]
16. Ferreira, G.M.; Fernandes, F.A.d.S.; Cavalcante, H.P.; Teixeira, M.B. Characterization of the Mechanical Properties of Concrete with Addition of Bamboo Fiber-Porto Nacional/TO. *Int. J. Adv. Eng. Res. Sci.* **2019**, *6*, 209–216. [CrossRef]
17. Pereira, A.P.; Ferreira, G.M.; Teixeira, M.B.; Fernandes, F.A.d.S. Production of Non-Structural Concrete with Addition of Polyethylene Terephthalate Fiber (PET) in Porto Nacional-TO. *Int. J. Adv. Eng. Res. Sci.* **2019**, *6*, 372–378. [CrossRef]
18. Stochero, N.P.; de Souza Chami, J.O.R.; Souza, M.T.; de Moraes, E.G.; de Oliveira, A.P.N. Green Glass Foams from Wastes Designed for Thermal Insulation. *Waste Biomass Valorization* **2021**, *12*, 1609–1620. [CrossRef]
19. Khan, M.N.N.; Jamil, M.; Karim, M.R.; Zain, M.F.M.; Kaish, A.B.M.A. Filler Effect of Pozzolanic Materials on the Strength and Microstructure Development of Mortar. *KSCE J. Civ. Eng.* **2017**, *21*, 274–284. [CrossRef]
20. Ali, M.R.; Maslehuddin, M.; Shameem, M.; Barry, M.S. Thermal-Resistant Lightweight Concrete with Polyethylene Beads as Coarse Aggregates. *Constr. Build. Mater.* **2018**, *164*, 739–749. [CrossRef]
21. Hu, N.; Fu, F.; Luo, B.; Ye, Y.; Chen, D.; Ou, Z.; Li, J. Preparation, Characterization and Self-Foaming Mechanism of Total-Tailings-Based Foamed Glass-Ceramics. *Ceram. Int.* **2023**, *49*, 31881–31890. [CrossRef]
22. Fu, F.; Hu, N.; Ye, Y.; Chen, G. The Foaming Mechanism and Properties of SiO_2–Al_2O_3–CaO-Based Foamed Ceramics with Varied Foaming Agents. *Ceram. Int.* **2023**, *49*, 32448–32457. [CrossRef]
23. Zhu, M.; Ji, R.; Li, Z.; Wang, H.; Liu, L.; Zhang, Z. Preparation of Glass Ceramic Foams for Thermal Insulation Applications from Coal Fly Ash and Waste Glass. *Constr. Build. Mater.* **2016**, *112*, 398–405. [CrossRef]
24. de Moraes, E.G.; Bigi, M.; Stochero, N.P.; Arcaro, S.; Siligardi, C.; Novaes de Oliveira, A.P. Vitrocrystalline Foams Produced with EPS as Pore Former: Processing and Characterization. *Process Saf. Environ. Prot.* **2019**, *121*, 12–19. [CrossRef]
25. Akerman, M. Introduçao Ao Vidro e Sua Produção. *ABIVIDRO-Esc. Vidro*. **2013**, 53. Available online: https://wikividros.eesc.usp.br/introducao_ao_vidro_e_sua_producao (accessed on 20 March 2024).
26. Souza, M.T.; Maia, B.G.O.; Teixeira, L.B.; de Oliveira, K.G.; Teixeira, A.H.B.; Novaes de Oliveira, A.P. Glass Foams Produced from Glass Bottles and Eggshell Wastes. *Process Saf. Environ. Prot.* **2017**, *111*, 60–64. [CrossRef]
27. Andrade Neto, J.d.S.; de França, M.J.S.; Amorim Júnior, N.S.d.; Ribeiro, D.V. Effects of Adding Sugarcane Bagasse Ash on the Properties and Durability of Concrete. *Constr. Build. Mater.* **2021**, *266*, 120959. [CrossRef]
28. França, S.; Sousa, L.N.; Saraiva, S.L.C.; Ferreira, M.C.N.F.; Silva, M.V.d.M.S.; Gomes, R.C.; Rodrigues, C.d.S.; Aguilar, M.T.P.; Bezerra, A.C.d.S. Feasibility of Using Sugar Cane Bagasse Ash in Partial Replacement of Portland Cement Clinker. *Buildings* **2023**, *13*, 843. [CrossRef]
29. Elmer, T.H.; Meissner, H.E. Increase of Annealing Point of 96% SiO_2 Glass on Incorporation of Carbon. *J. Am. Ceram. Soc.* **1976**, *59*, 206–209. [CrossRef]
30. Arif, E.; Clark, M.W.; Lake, N. Sugar Cane Bagasse Ash from a High-Efficiency Co-Generation Boiler as Filler in Concrete. *Constr. Build. Mater.* **2017**, *151*, 692–703. [CrossRef]
31. Zhou, J.F.J.; Xiao, Y.; Fung Kin Yuen, V.; Gözaydın, G.; Ma, X.; Panda, S.; Pham, T.T.; Yan, N.; Zhou, K. An Integrated Process for L-Tyrosine Production from Sugarcane Bagasse. *ACS Sustain. Chem. Eng.* **2021**, *9*, 11758–11768. [CrossRef]
32. Sua-iam, G.; Makul, N. Use of Increasing Amounts of Bagasse Ash Waste to Produce Self-Compacting Concrete by Adding Limestone Powder Waste. *J. Clean. Prod.* **2013**, *57*, 308–319. [CrossRef]
33. König, J.; Petersen, R.R.; Yue, Y.; Suvorov, D. Gas-Releasing Reactions in Foam-Glass Formation Using Carbon and Mn_xO_y as the Foaming Agents. *Ceram. Int.* **2017**, *43*, 4638–4646. [CrossRef]
34. König, J.; Petersen, R.R.; Yue, Y. Influence of the Glass–Calcium Carbonate Mixture's Characteristics on the Foaming Process and the Properties of the Foam Glass. *J. Eur. Ceram. Soc.* **2014**, *34*, 1591–1598. [CrossRef]
35. Fernandes, H.R.; Tulyaganov, D.U.; Ferreira, J.M.F. Preparation and Characterization of Foams from Sheet Glass and Fly Ash Using Carbonates as Foaming Agents. *Ceram. Int.* **2009**, *35*, 229–235. [CrossRef]
36. Zhou, M.; Ge, X.; Wang, H.; Chen, L.; Chen, X. Effect of the CaO Content and Decomposition of Calcium-Containing Minerals on Properties and Microstructure of Ceramic Foams from Fly Ash. *Ceram. Int.* **2017**, *43*, 9451–9457. [CrossRef]

37. Lamkin, M.A.; Riley, F.L.; Fordham, R.J. Oxygen Mobility in Silicon Dioxide and Silicate Glasses: A Review. *J. Eur. Ceram. Soc.* **1992**, *10*, 347–367. [CrossRef]
38. Pokorny, A.; Vicenzi, J.; Pérez Bergmann, C. Influence of Heating Rate on the Microstructure of Glass Foams. *Waste Manag. Res.* **2011**, *29*, 172–179. [CrossRef] [PubMed]
39. Lyra, G.P.; dos Santos, V.; De Santis, B.C.; Rivaben, R.R.; Fischer, C.; Pallone, E.M.d.J.A.; Rossignolo, J.A. Reuse of Sugarcane Bagasse Ash to Produce a Lightweight Aggregate Using Microwave Oven Sintering. *Constr. Build. Mater.* **2019**, *222*, 222–228. [CrossRef]
40. Rezvani, S.; Chuo, Y.S.; Lee, J.; Park, S.S. Hybrid Sintering of CNT/PZT Ceramics Using Microwave Oven. *Ceram. Int.* **2022**, *48*, 14684–14696. [CrossRef]
41. Batienkov, R.V.; Bol'shakova, A.N.; Khudnev, A.A. Microwave Sintering of Metal Powder Materials (Review). *Metallurgist* **2021**, *65*, 82–91. [CrossRef]
42. Ramesh, S.; Zulkifli, N.; Tan, C.Y.; Wong, Y.H.; Tarlochan, F.; Ramesh, S.; Teng, W.D.; Sopyan, I.; Bang, L.T.; Sarhan, A.A.D. Comparison between Microwave and Conventional Sintering on the Properties and Microstructural Evolution of Tetragonal Zirconia. *Ceram. Int.* **2018**, *44*, 8922–8927. [CrossRef]
43. Rossignolo, J.A.; Borrachero, M.V.; Soriano, L.; Payá, J. Influence of Microwave Oven Calcination on the Pozzolanicity of Sugar Cane Bagasse Ashes (SCBA) from the Cogeneration Industry. *Constr. Build. Mater.* **2018**, *187*, 892–902. [CrossRef]
44. Setayesh Gar, P.; Suresh, N.; Bindiganavile, V. Sugar Cane Bagasse Ash as a Pozzolanic Admixture in Concrete for Resistance to Sustained Elevated Temperatures. *Constr. Build. Mater.* **2017**, *153*, 929–936. [CrossRef]
45. König, J.; Petersen, R.R.; Yue, Y. Fabrication of Highly Insulating Foam Glass Made from CRT Panel Glass. *Ceram. Int.* **2015**, *41*, 9793–9800. [CrossRef]
46. Petersen, R.R.; König, J.; Yue, Y. The Viscosity Window of the Silicate Glass Foam Production. *J. Non. Cryst. Solids* **2017**, *456*, 49–54. [CrossRef]
47. Talybly, I.A.; Samedzade, G.M.; Masyeva, L.F.; Mammadov, A.N.; Gasimova, A.M.; Shadlinskaya, G.B. Modeling the Process of Granulation of Dusty-Type Clay with Dipper Method on a Pelletizing Granulator. *Chem. Probl.* **2020**, *18*, 68–77. [CrossRef]
48. de Moraes, E.G.; Sangiacomo, L.; Stochero, N.P.; Arcaro, S.; Barbosa, L.R.; Lenzi, A.; Siligardi, C.; Novaes de Oliveira, A.P. Innovative Thermal and Acoustic Insulation Foam by Using Recycled Ceramic Shell and Expandable Styrofoam (EPS) Wastes. *Waste Manag.* **2019**, *89*, 336–344. [CrossRef]
49. Chuang, K.-H.; Lu, C.-H.; Chen, J.-C.; Wey, M.-Y. Reuse of Bottom Ash and Fly Ash from Mechanical-Bed and Fluidized-Bed Municipal Incinerators in Manufacturing Lightweight Aggregates. *Ceram. Int.* **2018**, *44*, 12691–12696. [CrossRef]
50. Dong, Y.; Guo, W.; Jiang, C.; Shao, Y.; Zhang, L.; Wang, D.; Lu, X.; Huang, S.; Cheng, X. Using CaO as a Modifier Agent to Optimize the Pore Structure of Foamed Ceramics from Granite Scrap. *Ceram. Int.* **2023**, *49*, 13443–13451. [CrossRef]
51. Vieira, A.P.; Toledo Filho, R.D.; Tavares, L.M.; Cordeiro, G.C. Effect of Particle Size, Porous Structure and Content of Rice Husk Ash on the Hydration Process and Compressive Strength Evolution of Concrete. *Constr. Build. Mater.* **2020**, *236*, 117553. [CrossRef]
52. Cao, W.; Cheng, X.; Gong, L.; Li, Y.; Zhang, R.; Zhang, H. Thermal Conductivity of Highly Porous Ceramic Foams with Different Agar Concentrations. *Mater. Lett.* **2015**, *139*, 66–69. [CrossRef]
53. Akai, T.; Fukumi, K.; Yamashita, M. Formation of Pale Foam Glass from Colored Glass Cullet. *J. Ceram. Soc. Jpn.* **2020**, *128*, 153–157. [CrossRef]
54. Cao, M.; Liu, Z.; Xie, C. Effect of Steel-PVA Hybrid Fibers on Compressive Behavior of $CaCO_3$ Whiskers Reinforced Cement Mortar. *J. Build. Eng.* **2020**, *31*, 101314. [CrossRef]
55. Toscano Miranda, N.; Lopes Motta, I.; Maciel Filho, R.; Wolf Maciel, M.R. Sugarcane Bagasse Pyrolysis: A Review of Operating Conditions and Products Properties. *Renew. Sustain. Energy Rev.* **2021**, *149*, 111394. [CrossRef]
56. Pan, Z.; Jia, J.; Ju, J.; Niu, C.; Liu, D. Fabrication and Characterization of Glassy Carbon Foams with Controllable Porosity and High Compressive Strength. *Diam. Relat. Mater.* **2023**, *138*, 110256. [CrossRef]
57. Han, Y.; Kim, H.; Park, J. Fabrication and Characterization of Macroporous Flyash Ceramic Pellets. *Mater. Charact.* **2011**, *62*, 817–824. [CrossRef]
58. Rossignolo, J.A.; Agnesini, M.V.C. Concreto Leve Estrutural. In *Concreto: Ciência e Tecnologia*; IBRACON: São Paulo, Brazil, 2011; Volume II, Chapter 42; pp. 1531–1568.
59. Bernardo, E.; Cedro, R.; Florean, M.; Hreglich, S. Reutilization and Stabilization of Wastes by the Production of Glass Foams. *Ceram. Int.* **2007**, *33*, 963–968. [CrossRef]
60. Spiridonov, Y.A.; Orlova, L.A. Problems of Foam Glass Production. *Glas. Ceram.* **2003**, *60*, 313–314. [CrossRef]
61. Mohammadhosseini, H.; Alyousef, R.; Tahir, M.M. Towards Sustainable Concrete Composites through Waste Valorisation of Plastic Food Trays as Low-Cost Fibrous Materials. *Sustainability* **2021**, *13*, 2073. [CrossRef]
62. Shendy, H.; Khater, G.A.; Shahien, M.G.; Ragab, A.H.; Hassan, A.A.; Zayed, A.M. Innovative Pathways to High-Performance Glass Ceramics: Harnessing Nature's Treasures with Chromium and Zirconium Nucleation Catalysts. *Constr. Build. Mater.* **2024**, *411*, 134745. [CrossRef]

63. Shendy, H.; Khater, G.A.; Shahien, M.G.; Zayed, A.M. Preparation of Innovative Glass-Ceramic Materials Based on Mica Schist within the CaO–MgO–Al_2O_3–SiO_2 System. *Open Ceram.* **2024**, *17*, 100545. [CrossRef]
64. Verma, D.K.; Tripathy, S.; Srivastav, P.P. Microwave Heating in Rice and Its Influence on Quality and Techno-Functional Parameters of Rice Compositional Components. *J. Food Compos. Anal.* **2024**, *128*, 106030. [CrossRef]